LIANG, Y., WANG, S., FAN, Y., YANG, X., XIE, Y. and FERNANDEZ, C. 2022. Joint state of charge and state of health estimation of lithium-ion battery using improved adaptive dual extended Kalman filter based on piecewise forgetting factor recursive least squares. In *Proceedings of the 4th Smart power and internet energy systems international conference 2022 (SPIES 2022): towards a net-zero carbon future, 9-12 December 2022, Beijing, China.* Piscataway: IEEE [online], pages 1923-1927. Available from https://doi.org/10.1109/spies55999.2022.10082478

Joint state of charge and state of health estimation of lithium-ion battery using improved adaptive dual extended Kalman filter based on piecewise forgetting factor recursive least squares.

LIANG, Y., WANG, S., FAN, Y., YANG, X., XIE, Y. and FERNANDEZ, C.

2022

Joint State of Charge and State of Health Estimation of Lithium-ion Battery Using Improved Adaptive Dual Extended Kalman Filter Based on Piecewise Forgetting Factor Recursive Least Squares

Yawen Liang
Graduate student of the School of Information Engineering
Southwest University of Science and Technology
Mianyang, China
473878159@qq.com

Shunli Wang
Professor of the School of Information Engineering
Southwest University of Science and Technology
Mianyang, China
wangshunli@swust.edu.cn

Yongcun Fan
Associate Professor of the School of Information Engineering
Southwest University of Science and Technology
Mianyang, China
8121064@qq.com

Xiao Yang
Graduate student of the School of Information Engineering
Southwest University of Science and Technology
Mianyang, China
501369370@qq.com

Yanxin Xie
Doctorate of the School of Information Engineering
Southwest University of Science and Technology
Mianyang, China
2386078920@qq.com

Carlos Fernandez
Professor of the School of Pharmacy and Life Sciences
Robert Gordon University
Aberdeen, UK
ec.fernandez@rgu.ac.uk

***Abstract*—This work aims to improve the accuracy of state of charge estimation for lithium-ion battery, as well as to accurately estimate state of health. This study presents a piecewise forgetting factor recursive least squares method based on integral separation with a second-order resistor-capacitor model and uses a novel adaptive filter based on error covariance correction on the conventional dual extended Kalman filter. The experiments show that the error of SOC estimation is less than 0.61% and the error of SOH is less than 0.09% under different complex conditions, the proposed method can effectively improve the estimation accuracy and robustness.**

Keywords—State of charge, state of health, lithium-ion battery, adaptive dual extended Kalman filter, piecewise forgetting factor, prior error covariance correction

I. INTRODUCTION

One of the hottest topics in lithium-ion batteries research is the state of charge (SOC) and state of health (SOH) estimation [1]. Unfortunately, neither of these can be measured directly and both must be derived from sensor signals using model-based methods [2]. These signals can be erroneous and noisy, which will introduce inaccuracies into the state estimation, thus the available battery capacity is limited [3]. In addition, the model-based methods assumes that the system noise is a fixed noise, and there is a truncation error in the iterative computation process [4]. However, compared with data-driven methods, model-based methods are widely used in practical applications with their computational simplicity, low cost of use, and high accuracy [5]. Therefore, It is crucial to improve the model-based approach to enable more accurate estimation of the lithium-ion batteries SOC and SOH. It not only can balance the differences between individual cells, optimize charging and discharging strategies, as well as prevent safety hazards, but also is an important means to fully utilize the performance of lithium-ion batteries [6].

In related studies in recent years, a widely used approach addresses these problems is the dual extended Kalman filter (DEKF). It contains two extended Kalman filters (EKFs), that simultaneously estimate both the lithium-ion battery states and parameters [7]. This means that this algorithm has all the limitations of the EKF. In addition, arbitrary adjustments of the noise covariance may over- or underestimate the measured values, leading to stable divergence or too noisy filter behavior, respectively [8]. In the latter and worst condition, the filter estimate becomes an open-loop prediction process since the Kalman gain is minimized [9]. Furthermore, The noise covariance is usually kept as constant to meet the real-time requirements of the BMS, which greatly affect the filter response [10].

To tackling these difficulties, in this study, considering that the DEKF-based SOC and SOH estimation approach greatly depends on the appropriate system noise parameters and Kalman gain, a novel error covariance correction-adaptive extended Kalman filter (ECC-AEKF) is proposed, which can effectively achieve the dynamic adjustment of the system noise characteristics, reducing the impact of erroneous error covariances on the prior estimation and obtain a more suitable Kalman gain by appropriately matching the prior error covariance and noise covariance. Meanwhile, considering that a single forgetting factor recursive least squares (FFRLS) is not suitable for time-varying systems, a method of a piecewise forgetting factor recursive least-squares (PFFRLS) based on integral separation is used to adaptively identify the parameters of the equivalent circuit model (ECM) in real-time. To validate the accuracy and robustness of the proposed methods, experiments are conducted in different complex conditions with other widely used filtering methods for comparison. The experiment demonstrates that the methods proposed has a good estimation effect, which accuracy and robustness far exceed those of other universal used methods.

A. Equivalent Circuit Model

Establishing an ECM is a prerequisite for applying a model-based approach to estimate the lithium-ion battery state [11]. There are many types of typical models, among which, the second-order resistor-capacitor (RC) network model has a simple structure and can better reflect the dynamic and static performance of the lithium-ion battery compared to the Thevenin model [12]. The second-order RC network model is shown in Fig. 1.

As shown in Fig. 1, R_0 is the series resistance; R_1 and R_2 are the two polarization internal resistances; C_1 and C_2 are the two polarization capacitances; U_1 and U_2 are the voltage of the two RC-elements R_1C_1, R_2C_2, respectively. U_{oc} and U_L are the open circuit voltage and load terminal voltage of the battery, respectively.

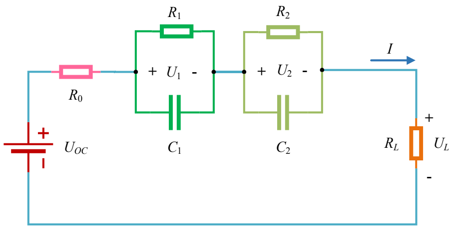

Fig. 1. Second-order RC network equivalent model

B. *The Piecewise Forgetting Factor Recursive Least Squares*

The forgetting factor is mainly used to increase the weight of new data, thereby enhancing the adaptability to non-stationary signals [13]. According to the characteristics of different sizes of forgetting factor, it can be regarded as the integration link in Proportion Integration Differentiation (PID) regulation. Therefore, a piecewise forgetting factor recursive least-squares (PFFRLS) method based on integral separation is constructed in this study, which is able to segment the forgetting factor according to the error between the current estimated output and the actual output. When the error is large, the integral action is canceled to avoid reducing the stability of the system. When the error is small, the integral action is introduced to eliminate the net difference and improve the control accuracy. Searching for several error points $\vartheta_1, \vartheta_2, \cdots \vartheta_n$ in the range of absolute errors, and when the error range is $[\vartheta_i, \vartheta_{i+1}]$, it corresponds to $\lambda = \lambda_i$, $i = 1,2,\cdots,n$, respectively. The correction function of λ is given in (1).

$$\lambda = \begin{cases} \lambda_1, \vartheta_1 \le |e| < \vartheta_2 \\ \lambda_2, \vartheta_2 \le |e| < \vartheta_3 \\ \vdots \\ \lambda_i, \vartheta_{i-1} \le |e| < \vartheta_i \end{cases} \tag{1}$$

From (1), the forgetting factor is adaptively adjusted by the absolute error between the current estimated output and the actual output. When the absolute error is large, a smaller forgetting factor is selected to improve the tracking speed of the estimated parameters when the parameters are abruptly changed. When the absolute error is small, a larger forgetting factor is selected, so that the parameters have better steady-state performance. The purpose of PFFRLS method is to accurately value the forgetting factor in real time, so as to ensure that the system has better stability and robustness.

The detail steps of the PFFRLS method can be summarized as follows:

Step 1. Initialize estimation parameter and error covariance at step $k = 0$.

$$\begin{cases} \hat{\theta}_0^+ = E(\theta_0) \\ z_0^+ = E[(\theta_0 - \hat{\theta}_0^+)(\theta_0 - \hat{\theta}_0^+)^T] \end{cases} \tag{2}$$

Step 2. Estimation of parameter and covariance update.

$$\begin{cases} \hat{\theta}_k^- = \hat{\theta}_{k-1}^+ \\ z_k^- = z_{k-1}^+ \end{cases} \tag{3}$$

Step 3. Calculation of algorithm gain.

$$L(k+1) = P(k)\varphi(k+1)[\lambda + \varphi^T(k+1)P(k)\varphi(k+1)]^{-1} \tag{4}$$

Step 4. Output prediction and estimation of error update.

$$\begin{cases} E(k) = \phi(k)\theta^T \\ e(k) = y(k+1) - \varphi^T(k+1)\hat{\theta}(k) \end{cases} \tag{5}$$

Step 5. Posteriori estimation of parameter and covariance update.

$$\begin{cases} \hat{\theta}(k+1) = \hat{\theta}(k) + L(k+1)e(k) \\ P(k+1) = \lambda^{-1}[P(k) - L(k+1)\varphi^T(k+1)P(k)] \end{cases} \tag{6}$$

where, the piecewise forgetting factor is calculated as (1).

II. JOINT SOC AND SOH ESTIMATION APPROACH

The Kalman gain is closely related to noise covariance and error covariance. A proper selection of the Kalman gain can decrease the estimation error. If the parameters of the lithium-ion battery change slowly during the operation of the system, the prior error covariance is convergent. Therefore, the estimation of the prior error covariance can be corrected in real time by finding a locally optimal but explicit and efficient way.

A. *The Improved Adaptive Dual Extended Kalman Filter*

In order to avoid the effect of artificially adjusted noise covariance on the error covariance and to reset an appropriate prior error covariance to obtain a more appropriate Kalman gain, an novel error covariance correction-based adaptive dual extended Kalman filter (ECC-ADEKF) is designed to find a new relationship between the prior error covariance and the state covariance by solving the maximum likelihood function of the probability density function of the error sequence conditional on the prior covariance. In this optimal adaptive estimator, the error sequence is the crucial data used to adaptively update the ECM parameters, which is defined as shown in (7).

$$e_k = y_k - h(\hat{x}_{k|k-1}, u_k) \tag{7}$$

The probability density function of the historical error sequence conditional on the prior covariance is shown in (8).

$$p(\xi_k | \hat{P}_{k|k-1}) = \frac{p(\{e_{i_0}, e_{i_0+1}, \cdots, e_{k-1}\})}{p(\hat{P}_{k|k-1})} = \prod_{i=i_0}^{k-1} p(e_i | \hat{P}_{k|k-1}) \tag{8}$$

where $\xi_k = \{e_{i_0}, e_{i_0+1}, \cdots, e_{k-1}\}$ represent the set of error sequences, $\hat{P}_{k|k-1}$ represent the estimated value of the prior error covariance, $p(e_i | \hat{P}_{k|k-1})$ represent the probability density function of the error sequence e_k conditional on the prior covariance $\hat{P}_{k|k-1}$.

By solving (8), a new recursive formula for estimating the prior error covariance can be obtained as shown in (9).

$$\hat{P}_{k|k-1} = \hat{P}_{k-1|k-2} + \frac{\Delta\hat{x}_{k-1}\Delta\hat{x}_{k-1}^T - L_{k-1}C_{k-1}\hat{P}_{k-1|k-2}}{k-i_0} \quad (9)$$

The detail steps of the ECC-ADEKF algorithm can be summarized as follows:

Step 1. Initialization of state variable and error covariance matrix.

$$\begin{cases} x_0 = E[x_0] \\ P_0 = E\left[(x_0 - x_0)(x_0 - x_0)^T\right] \end{cases} \quad (10)$$

Step 2. Update the state variables.

$$x_{k|k-1} = f(x_{k-1|k-1}, u_{k-1}) \quad (11)$$

Step 3. Update the state covariance at the filter convergence time k_0.

$$\begin{cases} \hat{P}_{k|k-1} = A_{k-1}P_{k-1|k-1}A_{k-1}^T + Q_k, k \le k_0 \\ \hat{P}_{k|k-1} = \hat{P}_{k-1|k-2} + \dfrac{\Delta\hat{x}_{k-1}\Delta\hat{x}_{k-1}^T - L_{k-1}C_{k-1}\hat{P}_{k-1|k-2}}{k-i_0}, k > k_0 \end{cases} \quad (12)$$

Step 4. Calculation of the Kalman gain.

$$L_k = P_{k|k-1}C_k^T(C_kP_{k|k-1}C_k^T + R_k)^{-1} \quad (13)$$

where Q_k and R_k are the covariances of the process noise and the measurement noise, respectively.

Step 5. Estimation of the state variables and error covariance.

$$\begin{cases} x_{k|k} = x_{k|k-1} + L_k\left[y_k - g(x_{k|k-1}, u_k)\right] \\ P_{k|k} = (E - K_kC_k)P_{k|k-1} \end{cases} \quad (14)$$

The ECC-ADEKF algorithm contains two ECC-AEKFs, that simultaneously estimate both the lithium-ion battery SOC and SOH. The optimization algorithm obtains the functional relationship between the feedback information $\Delta\hat{x}_i$ and the prior error covariance $P_{k|k-1}$ through the maximum likelihood method. Further, the statistical characteristics of the process noise can be indirectly estimated. The appropriate Kalman gain is obtained by adjusting the matching relationship between the prior error covariance and the noise covariance.

The proposed algorithm has some limitations. Its derivation is suboptimal due to it presupposes the condition that the prior error covariances of the SOC estimation process are approximate in the steady state. In addition, this experiment was performed at room temperature and did not involve the analysis of temperature variations, which can cause excess inaccuracy. However, this experiment shall be used as a simulated attempt to study the reliability of SOC estimation under conditions where accurate noise parameters are not available and applications, so as to further avoid the failure of Kalman gain due to over- or underestimation of noise covariance.

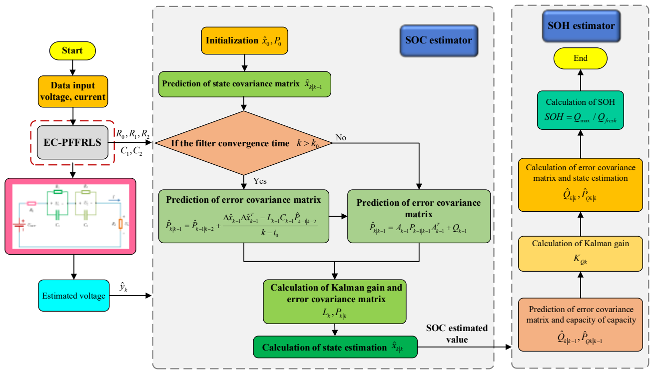

Fig. 2. The flowchart of the joint estimation with the proposed methods

B. Schematic of the Joint SOC and SOH Estimation

The joint estimation method proposed in this study includes the PFFRLS identification method and the ECC-ADEKF algorithm. The flowchart of the joint estimation based on proposed methods is shown in Fig. 2.

III. Results and Discussion

A. Battery Model Verification

This subsection verifies the accuracy of the model and the feasibility of the proposed identification method. The single forgetting factor λ is set as 0.99, 0.98, and 0.97, respectively. Fig. 3 shows the experimental results of the FFRLS method ($\lambda = 0.98$) and the PFFRLS method under DST condition.

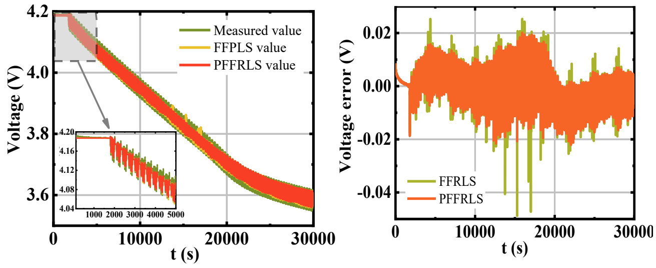

(a) Terminal voltage estimation results (b) Terminal voltage estimation error

Fig. 3. Model parameter identification results

The error properties corresponding to the two parameter identification methods under HPPC and DST conditions are shown in Table I, where MaxAE stands for maximum absolute error.

TABLE I. Error Discussion of Identification Results

Condition	method	MaxAE (%)	MAE (%)	RMSE (%)
HPPC	Single forgetting factor ($\lambda = 0.99$)	7.023	1.642	1.920
	Single forgetting factor ($\lambda = 0.98$)	11.034	1.878	2.130
	Single forgetting factor ($\lambda = 0.97$)	14.813	2.210	2.320
	PFFRLS	6.420	1.430	1.878
DST	Single forgetting factor ($\lambda = 0.99$)	4.874	1.342	1.291
	Single forgetting factor ($\lambda = 0.98$)	8.435	1.537	1.813
	Single forgetting factor ($\lambda = 0.97$)	17.175	2.340	6.50
	PFFRLS	1.756	0.52	1.210

From Fig. 3 and Table I, under the DST condition, the accuracy of the PFFRLS method is better than the FFRLS method, with the smallest error. Moreover, the error of a

FFRLS increases as the forgetting factor decreases. The identification process of each parameter for the model based on the PFFRLS method is shown in Fig. 4.

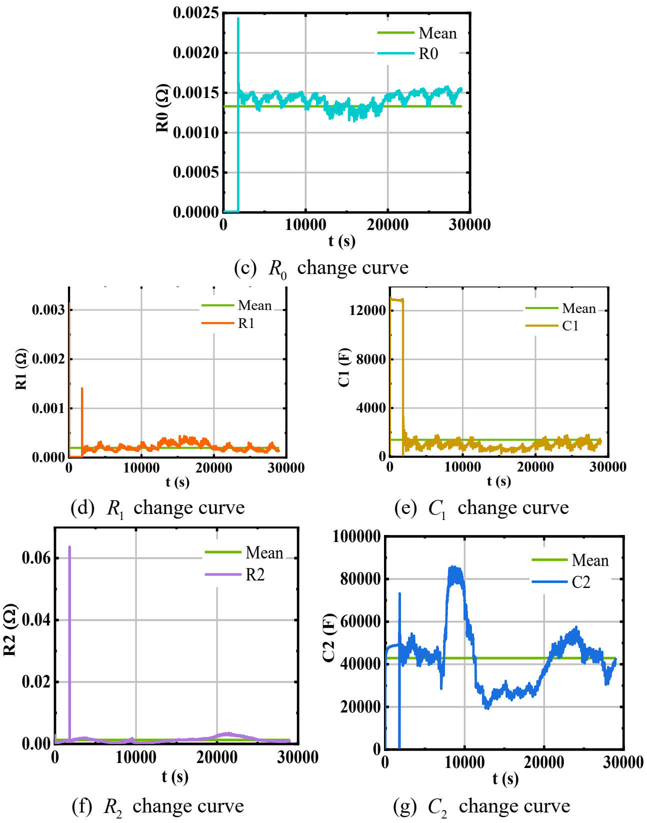

(c) R_0 change curve

(d) R_1 change curve (e) C_1 change curve

(f) R_2 change curve (g) C_2 change curve

Fig. 4. The identification process of each parameter

Fig. 4 indicates that under the DST condition, the PFFRLS method can quickly follow the real-time changes of model parameters, and effectively achieve accurate model identification. This shows that the established ECM has high accuracy and can better reflect the output characteristics of lithium-ion battery.

B. SOC Estimation

In this subsection, the effectiveness of the PFFRLS-ECC-ADEKF method is verified under the HPPC and DST conditions. Among then, the initial value of SOC was set to the correct value (100%). The proposed method is compared with the EKF and DEKF under offline identification, as well as the FFRLS-DEKF method ($\lambda = 0.98$). The SOC estimation results of the lithium-ion battery under HPPC and DST conditions are shown in Fig. 5 and Fig. 6, respectively.

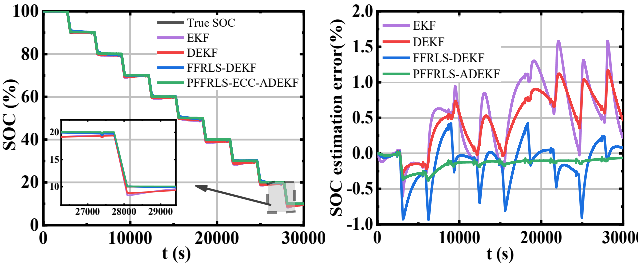

(a) SOC estimation change curves (b) SOC estimation errors

Fig. 5. SOC estimation results under HPPC condition

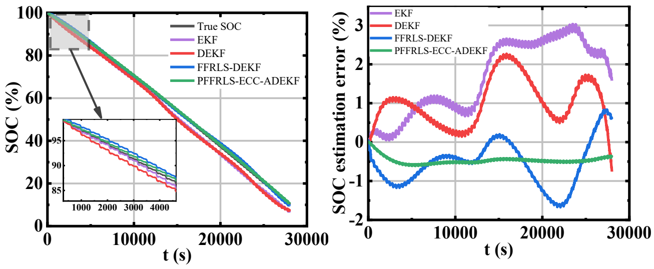

(a) SOC estimation charge curves (b) SOC estimation errors

Fig. 6. SOC estimation results under DST condition

The error properties corresponding to the four algorithms under HPPC and DST conditions are shown in TABLE II, where TC stands for time cost.

TABLE II. PERFORMANCE EVALUATION OF THE SOC ESTIMATION METHODS

Condition	method	SOC error (%)			
		MaxAE (%)	*MAE (%)*	*RMSE (%)*	*TC (s)*
HPPC	EKF	1.58	0.56	0.70	0.20
	DEKF	1.16	0.49	0.59	1.19
	FFRLS-DEKF ($\lambda = 0.98$)	0.94	0.21	0.30	3.11
	PFFRLS-ECC-ADEKF	0.38	0.13	0.16	1.53
DST	EKF	3.03	1.65	1.91	0.16
	DEKF	2.27	1.02	1.18	1.01
	FFRLS-DEKF ($\lambda = 0.98$)	1.68	0.67	0.80	1.33
	PFFRLS-ECC-ADEKF	0.61	0.47	0.48	1.43

From Fig. 5, Fig. 6, and Table II, the MaxAE, MAE, and RMSE of the EKF algorithm are the highest among the four algorithms. Compared with the DEKF algorithm under offline identification, the one under online identification has improved estimation accuracy, but the time cost is also increased. The proposed method has the best SOC estimation effect, which almost coincides with the SOC true value curve. It has better accuracy and stability, and besides, the time cost is only slightly larger than that of algorithms under offline identification.

To check the robustness of the proposed method, the initial values of SOC are set to 0.9, 0.8, and 0.7, and they are compared with the FFRLS-DEKF method ($\lambda = 0.98$) under DST condition. The experimental results of the robustness comparison are plotted in Fig. 7.

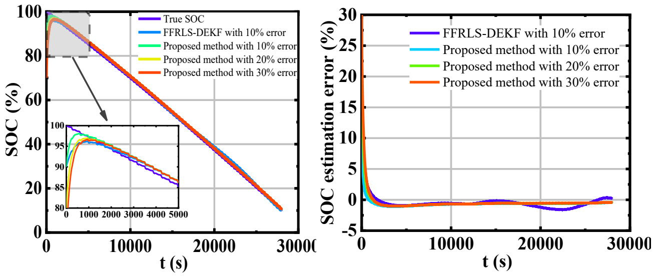

(a) SOC estimation change curves (b) SOC estimation errors

Fig. 7. SOC estimation results under DST condition with inistial error

By analyzing Fig. 7, it can be seen that when the initial value of SOC was not the correct value (100%), the proposed method can converge to approximately 0 in a faster way, and has better robustness.

C. SOH Estimation

In this subsection, the reasonableness and accuracy of the SOH estimation under PFFRLS-ECC-ADEKF method is verified on the basis of part IV-B. The SOH estimation results are shown in Fig. 8 and Fig. 9, respectively.

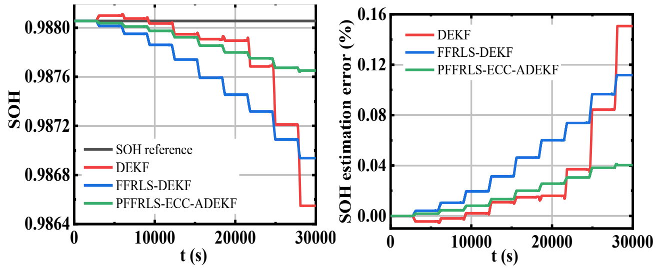

(a) SOH estimation change curves (b) SOH estimation errors

Fig. 8. SOH estimation results under HPPC condition

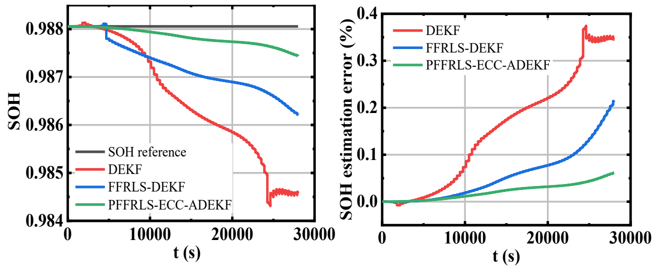

(a) SOH estimation change curves (b) SOH estimation errors

Fig. 9. SOH estimation results under DST condition

The error properties corresponding to the three algorithms under HPPC and DST conditions are shown in Table III.

TABLE III. PERFORMANCE EVALUATION OF THE SOH ESTIMATION METHODS

Condition	method	SOH error (%)			
		MaxAE (%)	*MAE (%)*	*RMSE (%)*	*TC (s)*
HPPC	DEKF	0.15	0.03	0.05	1.19
	FFRLS-DEKF ($\lambda = 0.98$)	0.09	0.02	0.03	3.11
	PFFRLS-ECC-ADEKF	0.04	0.01	0.02	1.53
DST	DEKF	0.37	0.15	0.19	1.01
	FFRLS-DEKF ($\lambda = 0.98$)	0.21	0.06	0.07	1.33
	PFFRLS-ECC-ADEKF	0.05	0.02	0.02	1.43

By analyzing Fig. 8, Fig. 9, and Table III, it can be seen that accurate SOH estimation relies on high precision SOC estimation to a large extent. Among them, the DEKF algorithm based on offline identification has the worst estimation, which its MaxAE, MAE, and RMSE are the highest among the three compared algorithms. Compared with that, the one under online identification has improved estimated effect, but still not the most desirable result. The proposed method has better SOH estimation, which not only has the lowest MaxAE, MAE, and RMSE among the three, but also has a TC with little difference from the EKF.

IV. CONCLUSION

In this study, the state and internal variable capacitance of the lithium-ion battery model have been estimated using an ECC-ADEKF method. This method is not limited to a single Kalman gain for iterative calculation, which can dynamically adjust the system noise characteristics, reducing the impact of erroneous error covariances on prior estimation and obtain a more appropriate Kalman gain to improve the accuracy and robustness of SOC estimation. In addition, the PFFRLS method based on integral separation is proposed for the parameter identification of the ECM, which has the advantage of adaptively identify the parameters in real-time. The simulations show that the error of SOC estimation is less than 0.61% and the error of SOH is less than 0.09% under different complex conditions. Therefore, compared with other commonly used model-based methods, the proposed method has superior joint SOC and SOH estimated results.

ACKNOWLEDGMEN

The work is supported by the National Natural Science Foundation of China (No. 62173281, 61801407), Sichuan Science and Technology Program (No. 2019YFG0427), China Scholarship Council (No. 201908515099), and Fund of Robot Technology used for Special Environment Key Laboratory of Sichuan Province (No. 18kftk03).

REFERENCES

[1] Xu, Y., et al., *State of charge estimation for lithium-ion batteries based on adaptive dual Kalman filter.* Applied Mathematical Modelling, 2020. 77: p. 1255-1272.

[2] Han, X., et al., *A review on the key issues of the lithium ion battery degradation among the whole life cycle.* 2019. 1: p. 100005.

[3] How, D.N., et al., *State of charge estimation for lithium-ion batteries using model-based and data-driven methods: A review.* Ieee Access, 2019. 7: p. 136116-136136.

[4] Yang, B., et al., *Classification, summarization and perspectives on state-of-charge estimation of lithium-ion batteries used in electric vehicles: A critical comprehensive survey.* Journal of Energy Storage, 2021. 39: p. 102572.

[5] Meng, J., et al., *Overview of lithium-ion battery modeling methods for state-of-charge estimation in electrical vehicles.* Applied sciences, 2018. 8(5): p. 659.

[6] Wang, Y., et al., *A comprehensive review of battery modeling and state estimation approaches for advanced battery management systems.* Renewable and Sustainable Energy Reviews, 2020. 131: p. 110015.

[7] Tian, H., et al., *A review of the state of health for lithium-ion batteries: Research status and suggestions.* Journal of Cleaner Production, 2020. 261: p. 120813.

[8] Vidal, C., et al., *Machine learning applied to electrified vehicle battery state of charge and state of health estimation: State-of-the-art.* IEEE Access, 2020. 8: p. 52796-52814.

[9] Li, X., et al., *State of health estimation for Li-Ion battery using incremental capacity analysis and Gaussian process regression.* Energy, 2020. 190: p. 116467.

[10] Wassiliadis, N., et al., *Revisiting the dual extended Kalman filter for battery state-of-charge and state-of-health estimation: A use-case life cycle analysis.* Journal of Energy Storage, 2018. 19: p. 73-87.

[11] Ali, M.U., et al., *Towards a smarter battery management system for electric vehicle applications: A critical review of lithium-ion battery state of charge estimation.* Energies, 2019. 12(3): p. 446.

[12] Hu, X., et al., *State estimation for advanced battery management: Key challenges and future trends.* Renewable and Sustainable Energy Reviews, 2019. 114: p. 109334.

[13] Shrivastava, P., et al., *Combined state of charge and state of energy estimation of lithium-ion battery using dual forgetting factor-based adaptive extended Kalman filter for electric vehicle applications.* IEEE Transactions on Vehicular Technology, 2021. 70(2): p. 1200-1215